PROCEEDINGS OF SPIE

SPIEDigitalLibrary.org/conference-proceedings-of-spie

Optical anisotropy due to perpendicular azimuth serial bideposition

Matthew C. Tai, Angus R. Gentle, Matthew D. Arnold, Geoffrey B. Smith

Matthew C. Tai, Angus R. Gentle, Matthew D. Arnold, Geoffrey B. Smith, "Optical anisotropy due to perpendicular azimuth serial bideposition," Proc. SPIE 10356, Nanostructured Thin Films X, 103560L (30 August 2017); doi: 10.1117/12.2273528

Event: SPIE Nanoscience + Engineering, 2017, San Diego, California, United States

SPIE.

Downloaded From: https://www.spiedigitallibrary.org/conference-proceedings-of-spie on 9/2/2018 Terms of Use: https://www.spiedigitallibrary.org/terms-of-use

Optical anisotropy due to perpendicular azimuth serial bideposition

Matthew C. Tai[a], Angus R. Gentle[a], Matthew D. Arnold[a], Geoffrey B. Smith[a]
[a]Institute for Nanoscale Technology, School of Mathematics and Physical Sciences, University of Technology Sydney, PO Box 123 Broadway NSW 2007, Sydney, Australia

ABSTRACT

Angled columnar structures produced by oblique angle deposition possess useful optical polarization effects. It is well known that this is due to structural anisotropy but the relative contributions of factors affecting this anisotropy are not fully understood in all cases. Serial bideposited films where the azimuth is changed during deposition can have greater birefringence if the azimuths are directly opposed. In contrast, in this article the properties of perpendicular azimuth films are studied: silicon films at tilt angles 50-80° were deposited and analyzed. Electron microscopy confirmed that the silicon nanostructures were formed off-axis, meaning they did not develop along the deposition axes but followed the averaged azimuth. Optical measurements confirm that the maximum birefringence occurs closer to glancing angles, and optical modelling demonstrates that in contrast to fixed azimuth films the birefringence in these perpendicular azimuth films is primarily modulated by depolarization factors.

Keywords: anisotropy, serial bideposition, glancing angle deposition, off-axis, nanostructures, thin films.

1. INTRODUCTION

Coatings deposited at oblique angles form highly porous, randomly ordered structures that have potential application in selective filters [1], retarders [2], polarimeters [3], sensors [4, 5], supercapacitors [6] and anodes for batteries [7].

Understanding growth processes is useful for optimizing the deposition of these films. It is understood that initial nucleation of the deposited material on the surface of the substrate precedes the process of columnar growth, which is primarily maintained by shadowing effects [8]. Minimization of diffusion maximizes shadowing processes leading to strong columnar growth. Fixed angle deposition produces films with angled columns related to the tilt angle of deposition. Rotation of the substrate, simulating multidirectional vapour flux [9], allows production of a great variety of structures including rods and helical columns [10-15] that are useful for different applications. Since a diverse range of structures with various properties can be readily formed over large areas, exploring and optimizing this process has continued to attract attention.

Our focus in this article is the resulting optical anisotropy [16-18]. This is not only useful for applications requiring optical polarization, but full optical characterization is also a useful tool for determining and understanding structural anisotropy and hence other properties of these films. We briefly review some important findings on optical anisotropy.

Fixed angle deposition results in tilted columns with biaxial anisotropy that is optimized around 60~70° substrate tilt [17], with the latter finding being repeated in many studies where the substrate is also rotated. Slow rotation of the films forms helical structures that have circularly polarizing activity [19]. Rapid rotation forms vertical columns with no in-plane activity due to uniaxial alignment with the substrate normal. However, serial bideposition with rapid stepping between opposing azimuths has been shown to produce vertical columns and increase birefringence, both in otherwise fixed angle deposits where the columns are strongly broadened perpendicular to the deposition plane [9, 20], and with slow rotation which produces twisted columns[19]. There have been a number of studies seeking to further modify the growth and resulting optical anisotropy. In particular, a prior study exploited perpendicular azimuth deposition to produce off-axis films for spatially multiplexed polarization arrays: the onset of in-plane birefringence at high angles was noted but only basic optical data was presented [4]. It is the aim of this article to explore and understand the factors contributing to the optical anisotropy of these films.

The simplest theory for understanding the optical anisotropy of obliquely deposited films is effective medium approximations (EMA), where the structure is assumed to be much smaller than the wavelength of light so that response is an average. The effective permittivity tensor can be modelled by mean-dipole expressions which are functions of the fill-factor (or complementary porosity) and the averaged dipole depolarization tensor aligned with the columnar structure. Typically the depolarization is lowest along the columns and greatest in the deposition plane, consistent with the known depolarization of ellipsoids corresponding to observed columnar shapes [21]. The projection of anisotropy

Nanostructured Thin Films X, edited by Yi-Jun Jen, Akhlesh Lakhtakia, Tom G. Mackay, Proc. of SPIE Vol. 10356, 103560L · © 2017 SPIE · CCC code: 0277-786X/17/$18 · doi: 10.1117/12.2273528

Downloaded From: https://www.spiedigitallibrary.org/conference-proceedings-of-spie on 9/2/2018
Terms of Use: https://www.spiedigitallibrary.org/terms-of-use

depends primarily on the column angle but also the orientation of the growth and deposition planes which are usually (but not always) aligned. It is understood that optical anisotropy is typically maximized at medium fill-factors and when the anisotropy in the depolarization is maximized [22], but the relative contribution of these factors in real films has to be determined by fitting measured data to a model.

The measurement linked most closely to anisotropy is ellipsometry, and indeed the in-plane anisotropy can be directly determined from normal-incidence transmission ellipsometry. However, full determination of optical properties and contributing factors is greatly facilitated by additional measurements such as polarized transmission/reflection coefficients [3, 4, 20], column angle and morphology determined by electron microscopy and ideally by thickness and packing fraction estimates from imaging and deposition rate calibration. This data can then be fitted to a parameterized EMA enabling the determination of the full permittivity tensor, depolarization factors and refined estimates for packing fraction and orientation. In this work we apply this process to determine both the magnitude and the factors contributing to the optical anisotropy of perpendicular azimuth deposits as well as confirm the fitted birefringence.

2. EXPERIMENTAL DETAILS

The nanostructured materials were deposited onto glass and silicon substrates in an electron beam PVD system at tilt angles of 45°, 50°, 55°, 60°, 65°, 70° for fixed azimuth films and 50°, 55°, 63°, 75°, 77° and 80° for the perpendicular azimuth films.

Glass substrates were prepared by sonication in a water-detergent mix for approximately 20 minutes then rinsed with deionized water and dried with nitrogen. Silicon substrates were also sonicated though in acetone for approximately 20 minutes then in ethanol for 5 minutes, next rinsed with deionized water and finally dried with nitrogen. The silicon used for evaporation was taken from spare substrate wafers and also prepared with the same procedures, and broken into small pieces for evaporation from a graphite crucible.

The electron beam evaporation system was evacuated to pressures better than 5×10^{-5} Torr and the material gradually heated with the electron beam to stabilize the deposition rate, and then the shutter released to open the substrate to evaporant flux. Deposition rate was maintained through automated feedback from a quartz crystal monitor (QCM) to electron beam power, however the oblique angle at the substrates means that the QCM is not an absolute measure of thickness of the film because that is affected by both flux projection and porosity. The samples were allowed to cool for 20 minutes before the chamber was vented to reduce thermal hazards.

For perpendicular azimuth deposition, similar parameters were used but a water-cooled stepped motor rotated the stage during deposition. The substrate underwent repeated step rotation based on the QCM signal, with azimuths of 0° and 90° achieved by repeated 90° and 270° step rotations alternated every 4nm for approximately 80 revolutions equating to 600 nm.

Nanostructures deposited onto the silicon substrates were viewed in cross-section and top-down in a Zeiss Supra 55VP SEM at 10-15 kV SEM to measure column angle and thickness as well as confirm porosity and column formation. Ellipsometric measurements were conducted in a J.A. Woollam V-VASE Ellipsometer in the range 300-3000 nm at angles 15-75°. Reflectance and transmittance coefficients were measured in a PerkinElmer Lambda 950 spectrophotometer between 300-2500 nm at angles of 8°, 15°, 30°, 45°, 60° with the polarizer set at 0° and 90° for each angle. An effective medium (biaxial Bruggeman) model was fitted to the data using WVASE32 software to estimate depolarization, porosity, column angle and thickness. Micrographic measurements of column angle and thickness were used as starting values for the fit procedure.

3. RESULTS AND DISCUSSION

The morphology of the deposited films was confirmed by electron microscopy, mostly on silicon substrates to avoid beam bending and charging. Figure 1 displays the SBD films that were deposited at perpendicular azimuths and the columnar structures formed at 75° elevation angle. To confirm the directions of deposition a top-down image was taken of a piece of dust with shadows showing the deposition planes. Looking closely at the image, the direction of growth of the structures can be seen to not be in the same plane as the incoming flux. This is where the name off-axis comes from due to the disparity between the deposition and growth planes. However, the

Downloaded From: https://www.spiedigitallibrary.org/conference-proceedings-of-spie on 9/2/2018
Terms of Use: https://www.spiedigitallibrary.org/terms-of-use

primary purpose of imaging was to quantify the cross-section column angle, which as expected is closer to the substrate normal. This data is used in the optical model and refined as summarized later.

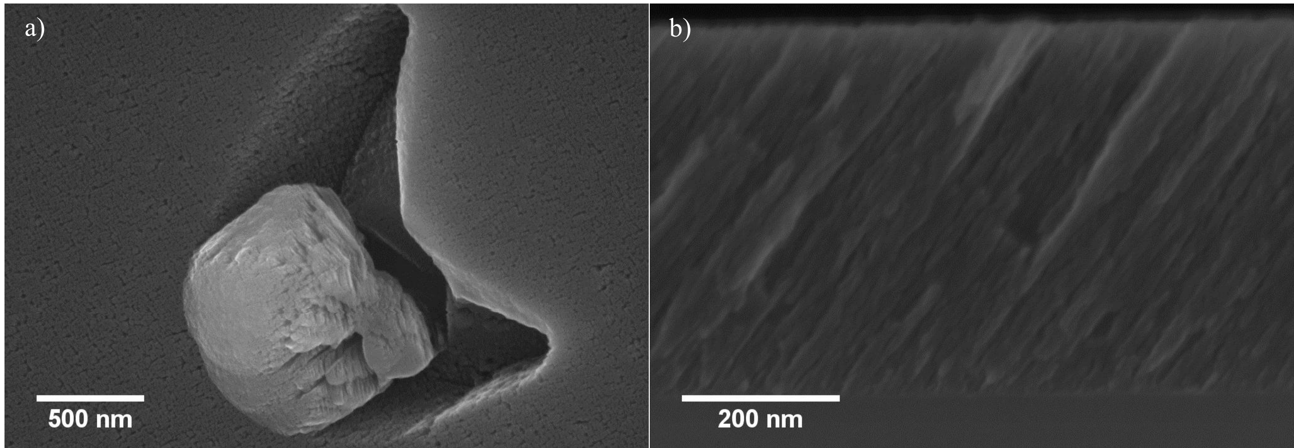

Figure 1 SEM micrograph of perpendicular azimuth deposit illustrating deposition planes: in plan view (a) the growth shadow due a contaminant particle shows in-plane azimuths and the cross-section view in (b) shows the column tilt.

Optical measurements were performed on films deposited on glass so that transmission measurements could be made. In particular, the normal in-plane birefringence (which is the most important data for polarizing filter applications) can be determined directly from normal-incidence transmission ellipsometry and independent thickness measurement. For fixed angle depositions maximum birefringence occurs between 50-60° (Figure 2a) which is expected, and as will be confirmed soon corresponds with increasing column angle and nearly optimal packing density – at high or low packing density the anisotropy must be minimized. In contrast, the perpendicular deposits (Figure 2b) have birefringence increasing to quite high angles and the birefringence is relatively small. This is consistent with a previous study but the reasons for it require a more thorough analysis.

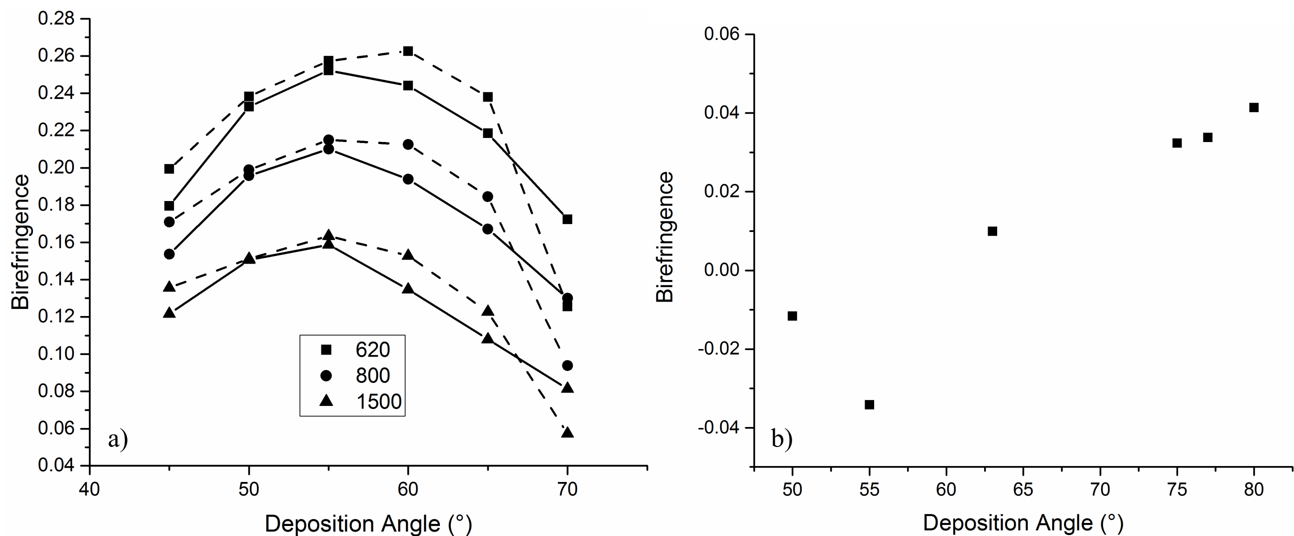

Figure 2 Birefringence of fixed angle with first (solid line) and second (dashed line) iterations at varying wavelengths (a) and perpendicular azimuth (b) deposits

Downloaded From: https://www.spiedigitallibrary.org/conference-proceedings-of-spie on 9/2/2018
Terms of Use: https://www.spiedigitallibrary.org/terms-of-use

To determine the full optical anisotropy and the importance of contributing factors, a wider range of measurements were combined and fitted to the EMA as outlined in the method. Some of the directly measured factors (e.g. column angle, thickness) were refined – this is justified on the basis that the properties of the deposits on silicon and glass substrates are expected to be similar but not necessarily exactly the same. Figure 3 illustrates the comparison between the parameters determined for fixed and perpendicular azimuth films.

Measurements were collated and imported into the WVASE32 software and an optical model was constructed based off the experimental data that was observed. The samples were fitted to multiple layers starting from glass at the bottom to the silicon film and layers that calculated the Bruggeman EMA. These films were classed as anisotropic and were fit corrected using the mean squared error (MSE). The biaxial Bruggeman effective media approximation was used to determine the packing densities and depolarization factors as well as the angles and rotation of the tensors to align with the grown structures. As this layer required initial guesses to be input into the software, estimates were obtained from known, measurable sources e.g. SEM was used to provide the starting values for thickness and column angle.

First we discuss the duplicated sets of fixed azimuth deposits (Figure 3 left-hand panels) which are relatively consistent. The depolarization factor in the z-direction (down the columns, L_z) and the x (L_x) and y (L_y) depolarization factors are the in-plane directions in the sample,

Figure 3 Fitted factors for fixed azimuth (left) and perpendicular azimuth (right) as a function of deposition angle. a & b) depolarization factors (inset of directions), c & d) column angle, e & f) packing densitya. has an inset that describes the directions of x,y and z when measured in the ellipsometer. The depolarization factors are relatively constant with angle, and the relative magnitudes are consistent with known results in that the depolarization along the columns (z) is small and the depolarization in the deposition plane (x) is large. The column angles in Fig 3c are quite consistent and follow a curve similar to the tangent rule as they increase with deposition angle. The only discrepancy to this trend with the column angle decreasing occurs at 70°. Figure 3e illustrates the expected trend of decreasing packing density of the columns due to greater self-shadowing.

The behavior of the perpendicular azimuth films (Figure 3 right hand panels) is substantially different. Overall, none of the parameters change very much with elevation angle. There are some outliers but these could be caused by the deposition conditions as the 63° sample had a decreased rate and was not deposited for as long as the other films. Due to the complexity of anisotropic films it is complicated to rigorously establish uncertainties, but the anisotropy of these films is relatively small which also may explain why experimental variations are more apparent. In general, the column angle in Figure 3d is closer to the normal than other types of films, the packing density is lower (Figure 3f) and the differences in depolarization are much smaller (Figure 3b).

The data as a whole suggests that the anisotropy of perpendicular azimuth films is probably dominated by small but consistent changes in the depolarization factors, since L_z and L_y swap over at about 60° corresponding to the onset of in-plane anisotropy seen in Figure 2b. This contrasts strongly with the results for fixed azimuth which are more strongly affected by packing density and possibly column angle. Replication of this experiment and comparison with other deposition regimes with different azimuth splits may help to elucidate general growth mechanisms in serial bideposition.

Downloaded From: https://www.spiedigitallibrary.org/conference-proceedings-of-spie on 9/2/2018
Terms of Use: https://www.spiedigitallibrary.org/terms-of-use

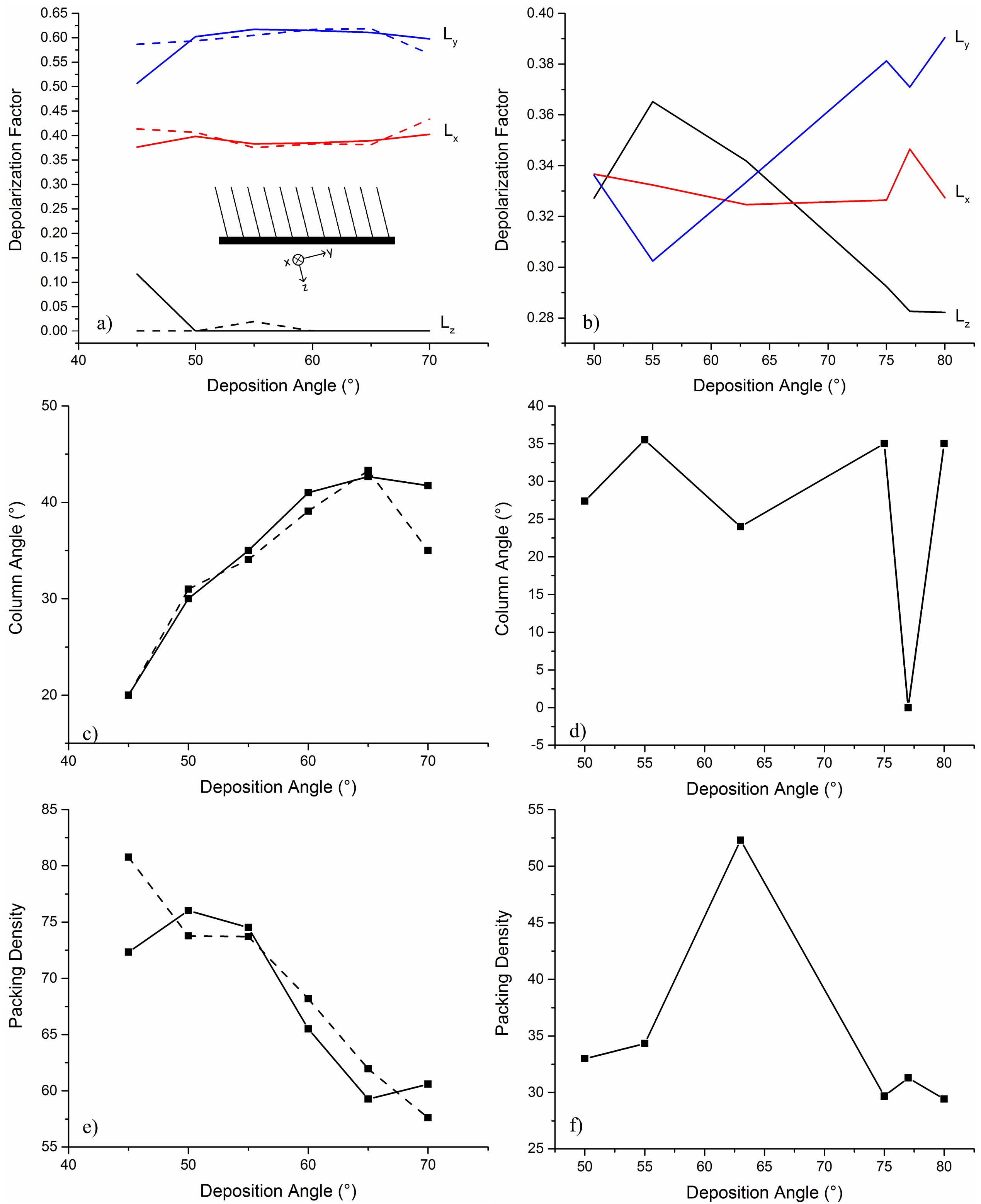

Figure 3 Fitted factors for fixed azimuth (left) and perpendicular azimuth (right) as a function of deposition angle. a & b) depolarization factors (inset of directions), c & d) column angle, e & f) packing density

Downloaded From: https://www.spiedigitallibrary.org/conference-proceedings-of-spie on 9/2/2018
Terms of Use: https://www.spiedigitallibrary.org/terms-of-use

4. CONCLUSION

Fixed and perpendicular azimuth obliquely deposited films were analyzed to determine which factors contribute strongly to birefringence in these films. In particular electron microscopy was used to determine column angle and optical modelling was then used to estimate packing density and effective depolarization factors. The parameters that affect the birefringence in these two regimes are fundamentally different with the perpendicular azimuth films being primarily affected by depolarization factors and the fixed azimuth films by column angle and packing density. Maximum in-plane birefringence occurred around 60° elevation for the fixed angle films consistent with previous studies, whereas birefringence only becomes significant in the perpendicular azimuth films after 63° due to the depolarization factors (L_z and L_y) changing in magnitude. The difference in these two regimes indicates that further study is necessary to fully understand the growth mechanisms affecting multi-azimuth deposition.

Downloaded From: https://www.spiedigitallibrary.org/conference-proceedings-of-spie on 9/2/2018
Terms of Use: https://www.spiedigitallibrary.org/terms-of-use

REFERENCES

[1] Q. H. Wu, L. D. Silva, M. Arnold *et al.*, "All-silicon polarizing filters for near-infrared wavelengths," Journal of Applied Physics, 95(1), 402-404 (2004).

[2] E. D. Walsby, M. Arnold, Q. h. Wu *et al.*, "Growth and characterisation of birefringent films on textured silicon substrates," Microelectronic Engineering, 78–79, 436-441 (2005).

[3] I. Hodgkinson, Q. hongWu, L. De Silva *et al.*, "Inorganic positive uniaxial films fabricated by serial bideposition," Optics Express, 12(16), 3840-3847 (2004).

[4] M. D. Arnold, I. J. Hodgkinson, Q. H. Wu *et al.*, "Multi-axis retarder arrays by masked oblique deposition," Journal of Vacuum Science & Technology B: Microelectronics and Nanometer Structures Processing, Measurement, and Phenomena, 23(4), 1398-1404 (2005).

[5] K. D. Harris, A. Huizinga, and M. J. Brett "High-Speed Porous Thin Film Humidity Sensors," Electrochemical and Solid-State Letters, 5(11), H27-H29 (2002).

[6] J. N. Broughton, and M. J. Brett "Electrochemical Capacitance in Manganese Thin Films with Chevron Microstructure," Electrochemical and Solid-State Letters, 5(12), A279-A282 (2002).

[7] P. R. Abel, Y.-M. Lin, H. Celio *et al.*, "Improving the Stability of Nanostructured Silicon Thin Film Lithium-Ion Battery Anodes through Their Controlled Oxidation," ACS Nano, 6(3), 2506-2516 (2012).

[8] D. Vick, L. J. Friedrich, S. K. Dew *et al.*, "Self-shadowing and surface diffusion effects in obliquely deposited thin films," Thin Solid Films, 339(1–2), 88-94 (1999).

[9] I. Hodgkinson, and Q. h. Wu, "Serial bideposition of anisotropic thin films with enhanced linear birefringence," Applied Optics, 38(16), 3621-3625 (1999).

[10] M. O. Jensen, and M. J. Brett, "Square spiral 3D photonic bandgap crystals at telecommunications frequencies," Optics Express, 13(9), 3348-3354 (2005).

[11] D. X. Ye, T. Karabacak, R. C. Picu *et al.*, "Uniform Si nanostructures grown by oblique angle deposition with substrate swing rotation," Nanotechnology, 16(9), 1717 (2005).

[12] K. Robbie, and M. J. Brett, "Sculptured thin films and glancing angle deposition: Growth mechanics and applications," Journal of Vacuum Science & Technology A: Vacuum, Surfaces, and Films, 15(3), 1460-1465 (1997).

[13] B. Dick, M. J. Brett, and T. Smy, "Investigation of substrate rotation at glancing incidence on thin-film morphology," Journal of Vacuum Science & Technology B: Microelectronics and Nanometer Structures Processing, Measurement, and Phenomena, 21(6), 2569-2575 (2003).

[14] S. R. Kennedy, M. J. Brett, O. Toader *et al.*, "Fabrication of Tetragonal Square Spiral Photonic Crystals," Nano Letters, 2(1), 59-62 (2002).

[15] K. D. Harris, K. L. Westra, and M. J. Brett "Fabrication of Perforated Thin Films with Helical and Chevron Pore Shapes," Electrochemical and Solid-State Letters, 4(6), C39-C42 (2001).

[16] S. Wang, G. Xia, H. He *et al.*, "Structural and optical properties of nanostructured TiO2 thin films fabricated by glancing angle deposition," Journal of Alloys and Compounds, 431(1–2), 287-291 (2007).

[17] T. Motohiro, and Y. Taga, "Thin film retardation plate by oblique deposition," Applied Optics, 28(13), 2466-2482 (1989).

[18] K. Robbie, L. J. Friedrich, S. K. Dew *et al.*, "Fabrication of thin films with highly porous microstructures," Journal of Vacuum Science & Technology A: Vacuum, Surfaces, and Films, 13(3), 1032-1035 (1995).

[19] I. Hodgkinson, Q. h. Wu, B. Knight *et al.*, "Vacuum deposition of chiral sculptured thin films with high optical activity," Applied Optics, 39(4), 642-649 (2000).

[20] G. Beydaghyan, K. Kaminska, T. Brown *et al.*, "Enhanced birefringence in vacuum evaporated silicon thin films," Applied Optics, 43(28), 5343-5349 (2004).

[21] I. J. Hodgkinson, and Q. Wu, [Birefringent Thin Films and Polarizing Elements], (1998).

[22] I. Hodgkinson, L. De Silva, and M. Arnold, "Inorganic polarizing materials grown by physical vapor deposition." 587001-587001-15.

Downloaded From: https://www.spiedigitallibrary.org/conference-proceedings-of-spie on 9/2/2018
Terms of Use: https://www.spiedigitallibrary.org/terms-of-use